Available online at www.sciencedirect.com
SCIENCE DIRECT®
Polymer 45 (2004) 2743–2750
polymer
www.elsevier.com/locate/polymer

Entropic model for the relaxation in vitreous systems. Estimation of uncertainty in the calculation of the conformational relaxation times

A. Saiter[a], J.M. Oliver[a,b], J.M. Saiter[a], J.L. Gómez Ribelles[b,*]

[a]*Laboratoire d'Etude et Caractérisation des Amorphes et des Polymères, Université de Rouen, Mont Saint Aignan 76821, France*
[b]*Center for Biomaterials and Department of Applied Thermodynamics, Universidad Politécnica de Valencia, Camino de Vera sn, E-46071 Valencia, Spain*

Received 2 May 2003; received in revised form 27 January 2004; accepted 11 February 2004

Abstract

Differential scanning calorimetry experiments were conducted on a thermotropic polyester. The experimental results consists of a series of thermograms measured on heating after different thermal histories that contained (or not) an isothermal stage at a temperature T_a below the glass transition with a duration t_a. The thermogram showed the characteristic peak in the region of the glass transition. The calculation of the relaxation times of the co-operative conformational rearrangements related to the glass transition and structural relaxation phenomena has been conducted by curve fitting using a phenomenological model. The curve fitting procedure was conducted simultaneously on a fixed number n of experimental thermograms. The aim of the paper is to present a method to estimate the uncertainty in the calculation of the model parameter. The results show how the computer simulated thermograms agree quite well to the experimental data. The uncertainty in the model parameters and through them the uncertainty in the calculated relaxation times is quite important when the number of experimental curves n is small but rapidly decreases as n increases and if more than five curves are used simultaneously in the fitting routine both the values of the model parameters and their uncertainty become independent on the number and thermal histories of the experimental thermograms.

Keywords: Glass transition; Structural relaxation; Polymer

1. Introduction

Differential scanning calorimetry is a suitable technique for the study of the conformational mobility of amorphous materials since it allows an accurate control of the thermal history of the sample

When an amorphous material (or an amorphous phase in a heterogeneous material) initially in equilibrium at a temperature T_1 is subjected to an instantaneous change of temperature until the temperature T_2, the response of the material has an instantaneous component (an instantaneous variation of the volume, enthalpy or entropy, elastic modulus, refraction index, dielectric permittivity etc.) and a delayed one, the latter is called the structural relaxation. In terms of the enthalpy, we will call $h^{eq}(T_1)$ the equilibrium value of the enthalpy at the temperature T_1, $h(T_2, 0)$ to the value reached immediately after the temperature step and $h(T_2, t)$ the value at time t. At infinity time $h(T_2, t)$ should reach the equilibrium value of the enthalpy at the temperature T_2, $h^{eq}(T_2)$. It has been proved that the kinetics of the structural relaxation can be characterised by a distribution of relaxation times in which the average relaxation time depends both on the temperature T_2 and on the value of the relaxing variable $h(T_2, t)$ (an equation based on a single relaxation time, even if it is dependent on the value of the enthalpy, cannot reproduce the well known experimental feature called memory effect). On the other hand a distribution of relaxation times depending only on the temperature is not able to reproduce the asymmetry of the relaxation process for positive and negative temperature jumps). The temperature dependence of the relaxation times follows the Vogel–Fulcher–Tamman–Hesse VFTH equation [1–3]. There is a narrow range of temperatures in which the values of the relaxation times attain the characteristic experimental times and then the glass transition is apparent. Below this temperature range the material is out of thermodynamical equilibrium immersed in the process that try and take it to the equilibrium state. Above the glass transition range the relaxation times are

* Corresponding author. Tel.: +34-933-877-275; fax: +34-963-877-276.
E-mail address: jlgomez@ter.up.es (J.L. Gómez Ribelles).

0032-3861/$ - see front matter © 2004 Published by Elsevier Ltd.
doi:10.1016/j.polymer.2004.02.014

short enough to allow the sample to reach the equilibrium state in a time interval shorter than the period needed to take any experimental datum and thus the observed state always corresponds to equilibrium. The glass transition appears thus as a consequence of the existence of the structural relaxation process. The glassy state is identified with the instantaneous response of the material and, in particular, the heat capacity at constant pressure in the glassy state is

$$c_{pg} = \frac{\partial[h^{eq}(T_1) - h(T_2, 0)]}{\partial(T_1 - T_2)}\Big)_p$$

while the heat capacity at constant pressure in the equilibrium liquid state is

$$c_{pl} = \frac{\partial[h^{eq}(T_1) - h^{eq}(T_2)]}{\partial(T_1 - T_2)}\Big)_p$$

The difference $\Delta c_p = c_{pl} - c_{pg}$ is the configurational heat capacity.

It is not possible to perform accurate isothermal experiments in DSC because the value of the changes in the enthalpy of the sample due to structural relaxation is not high enough. Instead, the specific heat of the sample is measured during a heating scan performed in a temperature interval that includes that of the glass transition. Previously the sample has been subjected to a thermal treatment that starts with the sample in equilibrium at a temperature well above the glass transition. This thermal treatment includes cooling at fixed rates and isothermal periods at temperature T_a (the annealing temperature) with duration t_a (annealing time). The thermograms measured after annealing shows a characteristic peak in the heat flow or the heat capacity. The position of this peak depends on the values of the annealing temperature and time. There is not a direct way to determine the relaxation times of the structural relaxation times from the experimental thermogram (as it could be made in dielectric or dynamic-mechanical experiments), instead it is necessary to build complicated nonlinear models to simulate the process suffered by the sample during the experiment. As the model equations contain the temperature and structure dependence of the relaxation times, the comparison between the model simulation and the experimental thermograms allows to determine the evolution of the relaxation times along the thermal profile of the experiment.

Several models have been extensively used for these calculations [3–12]. They use to contain four or five fitting parameters that characterise the dependence of the relaxation times with temperature and the relaxing variable (fictive temperature, entropy or enthalpy) and the shape of the relaxation function. The set of parameters can be determined by curve fitting, looking for the best agreement between the model simulated thermograms and the experimental ones. When the fitting routine is conducted for a single thermogram, it has been frequently found that the model parameters depend systematically on the thermal history, i.e. on T_a and t_a when the sample was subjected to annealing or on the cooling rate from equilibrium [13–18]. This is obviously unacceptable from the point of view of the theory as the relaxation times must be independent on the thermal history. This behaviour can be interpreted as the fail of some of the model assumptions but at least partially it comes from the fact that the model parameters are strongly correlated [5,9,11,12,14,19]. Average values were assumed sometimes to represent the behaviour of the material but the curve fitting method can be improved if various experimental thermograms are fitted simultaneously [10,11,16]. A different approach is to look for a characteristic of the experimental thermograms, which should depend only on one model parameter and that, as a consequence, allows to determine it independently from the rest. This is the case of the apparent activation energy at the glass transition temperature Δh^* in the Narayanawasmany–Moynihan model [3,4] that can be obtained from the dependence of the glass transition temperature on the cooling rate from equilibrium [20], or the determination of the structural parameter x using the peak-shift method [21,22], and recently the possibility of determining the β parameter of the stretched exponential from the shape of the temperature modulated differential scanning calorimetry, TMDSC [24].

There is few information in the literature about the uncertainty in the determination of these parameters and through them the uncertainty of the determination of the structural relaxation times [14,23]. The aim of this work is to propose a method to carry out this kind of study. The method proposed will be applied in this work in the case of the model proposed in reference [11], nevertheless it could be applied to other models as well.

Recently, the temperature modulated differential scanning calorimetry, TMDSC, has been used do provide a direct determination of the structural relaxation times from the calorimetric measure. It has been proven [25] that there is a good agreement in the case of polystyrene between the values of the relaxation times calculated from TMDSC and form conventional DSC using the model described below and a curve fitting procedure to determine the values of the model parameters.

1.1. Model based on the evolution of the configurational entropy

The model has been explained elsewhere and has been applied in different amorphous [11,12,26,27] and semicrystalline polymers [28], including polymer networks [29,30] and liquid-crystalline polymers [31], thus only the main equations will be included here.

The evolution of the configurational entropy during a thermal history that consists of a series of temperature jumps from T_{i-1} to T_i at time instants t_i, followed by

isothermal stages is given by:

$$S_c(t) = S_c^{lim}(T(t)) - \sum_{i=1}^{n}\left(\int_{T_{i-1}}^{T_i} \frac{\Delta c_p^{lim}(T)}{T} dT\right)\phi(\xi - \xi_{i-1}) \quad (1)$$

where ξ is the reduced time [4]:

$$\xi = \int_0^t \frac{dt'}{\tau(t')} \quad (2)$$

The function $\tau(t)$ is determined implicitly by the dependence of τ on T and S_c during the thermal history, a dependence which is assumed to obey the equation of Adam and Gibbs [32] extended to non-equilibrium states (as proposed by Scherer [7] and Hodge [8]):

$$\tau(T, S_c) = A \exp\left(\frac{B}{TS_c(\xi, T)}\right) \quad (3)$$

and the relaxation function is assumed to be a stretched exponential of the reduced time:

$$\phi(\xi) = \exp(-\xi^{\beta}) \quad (4)$$

$S_c^{lim}(T)$ represents the value of the configurational entropy attained in the physical ageing process at infinite time, and $\Delta c_p^{lim}(T)$ is defined through

$$S_c^{lim}(T_i) - S_c^{lim}(T_{i-1}) = \int_{T_{i-1}}^{T_i} \frac{\Delta c_p^{lim}(T)}{T} dT. \quad (5)$$

Thus, if T^* is a temperature above the glass transition region, for any temperature T, in the glass transition temperature interval or below it,

$$S_c^{lim}(T) = S_c^{eq}(T^*) + \int_{T^*}^{T} \frac{\Delta c_p^{lim}(T)}{T} dT, \quad (6)$$

with

$$S_c^{eq}(T) = \int_{T_2}^{T} \frac{\Delta c_p(T)}{T} dT \quad (7)$$

where $\Delta c_p(T)$ is the conformational heat capacity, here taken as the difference between the heat capacities of the liquid and the glass, $\Delta c_p(T) = c_{pl}(T) - c_{pg}(T)$ (a linear dependence of $\Delta c_p(T)$ with temperature has been assumed in this work) and T_2 is the Gibbs–DiMarzio [33] temperature at which the configurational entropy in the equilibrium liquid would vanish.

The phenomenological models of the structural relaxation usually assume that the state attained at infinite time in the structural relaxation process at a temperature T_a, can be identified with the extrapolation to T_a of the equilibrium line experimentally determined at temperatures above T_g [5–9]. When the models are based on the fictive temperature concept T_f this is simply a result of the identification of the limit of T_f at infinite time with T. In the context of the model used in this paper this means that:

$$S_c^{lim}(T) = S_c^{eq}(T). \quad (8)$$

However, it has been shown that the agreement between the model simulation and the experiments is highly improved when the model includes an assumption leading to values of $S_c^{lim}(T)$ significantly higher than those of $S_c^{eq}(T)$ [11,12,25–27,29–31], and the results in this work also support this idea. The definition of the curve $S_c^{lim}(T)$ introduces new adjustable parameters in the model. The shape shown in Fig. 1 has been chosen because it needs only one additional parameter δ (defined as shown in the figure).

2. Experimental

The semi-rigid polymer studied in this work, poly-(oxy(2,2-dialkypropane-1,3 diyl) carboxylbisphenyl-4,4′ dicarbonyl), abbreviated DP1.**3**, was synthesised in the Physical Chemistry laboratory of Duisburg by M.Hess e. a. The number '**3**' indicates the number of carbons of the side chain attached to the tertiary carbon of the propyl spacer. The molar masses of this polymer were determined with size exclusion chromatography in line with multi angle laser light scattering. The results are $\langle M_w \rangle = 36500$ g/mol and $\langle M_n \rangle = 7200$ g/mol.

The calorimetric experiments were performed in a Perkin–Elmer DSC7 on a single encapsulated sample. The thermograms were recorded only on heating, after subjecting the sample to a thermal treatment that started at 423 K with the sample in equilibrium. In a series of experiments the sample was first cooled at 20 K/min to the annealing temperature of 353 K, kept at this temperature for a time t_a and cooled again at 20 K/min to 303 K, the heating scan followed at 20 K/min. Six of these experiments were conducted with annealing times 8040, 4800, 1330, 850, 480, and 120 min. (The recorded thermograms will be designed

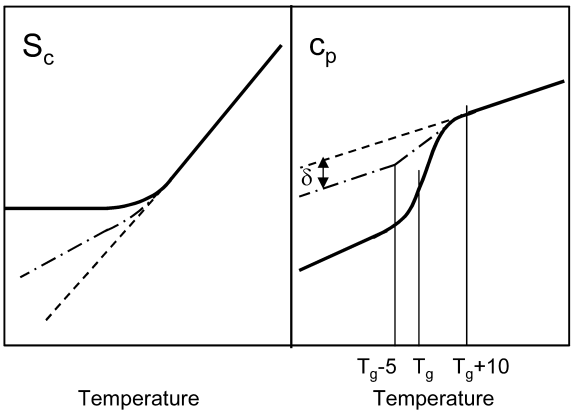

Fig. 1. (a) Sketch of the configurational entropy corresponding to the liquid state (dashed line), to an experimental cooling scan at a finite cooling rate (solid line), and to the hypothetical line of the limit states of the structural relaxation process (dashed-dotted line). (b) $c_p(T)$ lines corresponding to the three cases described in (a): the dashed line corresponds to the liquid state $c_{pl}(T)$ the solid line corresponds to an experimental cooling scan, and the dashed-dotted line corresponds to the specific heat capacity in the limit states of the structural relaxation process: $c_p^{lim}(T)$. The fitting parameter d, shown in the figure characterizes the difference between the slopes of the $S_c^{eq}(T)$ and $S_c^{lim}(T)$ lines below the glass transition.

by consecutive number A to F, respectively). In addition three experiments were conducted in which the sample was cooled from 423 to 303 K at different cooling rates q^- and then the thermogram was recorded on heating at 20 K/min. The thermograms recorded after thermal histories of this type with $q^- = 1$, 20 and 50 K/min will be called with numbers *G*, *H* and *I* respectively.

3. Results

The nine thermograms are represented in Fig. 2, showing the well known behaviour reported in many amorphous, semicrystalline and liquid-crystalline polymers for this type of experiments. The experimental curves are shown by circles and the full lines correspond to the curve calculated by the model. The peak shown in the thermogram shifts towards high temperatures and grows as the annealing time increases.

The decrease of the cooling rate also produces a

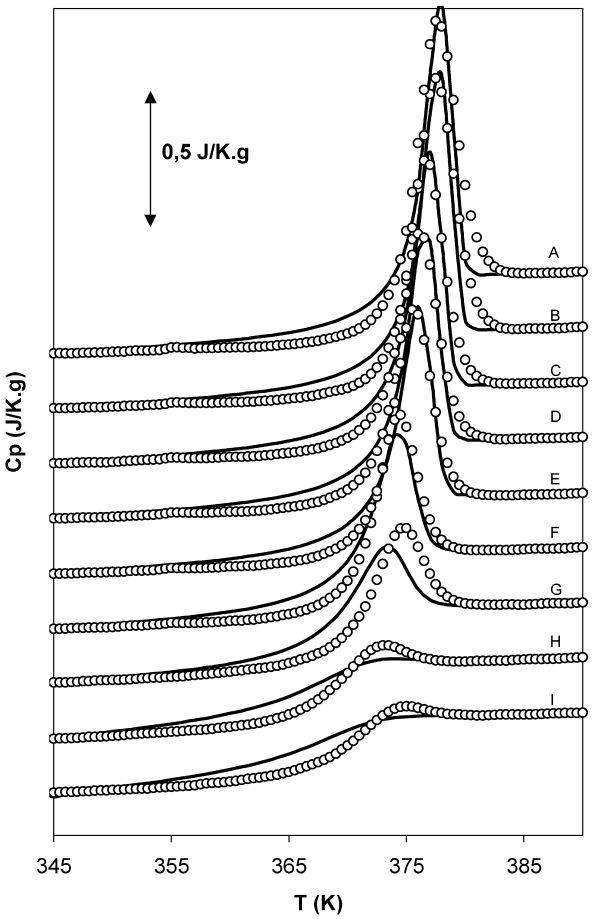

Fig. 2. Experimental thermograms measured on heating. The experimental curves are shown by circles and the full lines correspond to the curve calculated by the model. The thermal treatments before the measuring scan were as follows: (A to F) thermograms measured after annealing at 353 K for 8040, 4800, 1330, 850, 480 and 120 min respectively, (*G* to *I*) thermograms measured after cooling the sample from 423 to 303 K at 1, 20 and 50 K/min, respectively.

significant overshot in the thermogram. The temperature of the peak when the sample is cooled at 20 K min^{-1} is around 1.6 K below that of the peaks measured after cooling at 1 and 50 K min^{-1} which are quite close to each other. This feature has been described in the literature [6,12,34] it is also clear in the results of reference [31] and although not shown explicitly in the papers it is also clear in the results obtained in very different polymer systems which were studied in references [11,25–27,29,30]. The temperature of the peak shown in the heating thermogram first decreases as the cooling rate increases from very low values, goes through a minimum and increases again for increasing values of the heating rate. The differences in the temperature of the maximum are small: between 1 and 2° for cooling rates varying between 0.5 and 50 K min^{-1} in the polymers mentioned above.

3.1. Curve fitting. Determination of the uncertainty in the model parameters

It has been reported many times that in this model there is a strong correlation between the model parameters, specially between *B* and T_2, i.e., there are several sets of model parameters which yield the same model calculated thermograms. Thus, the first step in the fitting procedure was to conduct the least-squares search routine with fixed values of parameter *B*. In this step the nine experimental thermograms were fitted simultaneously. To do that the objective function to be minimised was

$$\mathrm{EC} = \sum_{i=1}^{9} \sum_{j=1}^{xxx} \frac{(X_{ij} - x_{ij})^2}{X_{ij}} \tag{9}$$

were X_{ij} is the *j*-sm experimental value measured in the thermogram *i* and x_{ij} is the value calculate with the model equations for the same temperature and thermal history. The quadratic error was divided by the experimental value in order to decrease the importance of the points around the maximum. When this correction is not included the fit of the low-temperature side of the transition can be poorer with no significant benefit in the fit of the position at height of the maximum.

Table 1 shows the sets of parameters δ, β, T_2 and $\ln A$ that gives the minimum value of the error function for different values of *B*. The curves calculated with the model equations with $B = 550$ J/g and the rest of parameters according to Table 1 are represented by the full lines in Fig. 2. As the fit of the experimental result to the model equations is not perfect, the search routine tends to find a solution in which the error in the fit of thermograms with small or no peaks is much higher than the error in those with higher values of the heat flow because in this way the total error is smaller. Thus, in the case of the nine thermograms represented in Fig. 2, the thermograms *G*, *H* and *I* (In fact *H* and *I*, corresponding to cooling from equilibrium at 20 and 50 K/min are nearly identical) are quite poorly fitted. On the

Table 1
Model parameters (δ, β, T_2, ln A) found by simultaneous curve fitting of the nine experimental thermograms, keeping the value of B fixed. The value of the error function (EC), the apparent activation enthalpy in equilibrium at T_g($\Delta h^*/R$) and the fragility parameter (m) are also included

B (J/g)	δ	β	T_2 (°C)	Ln(A/s)	EC	$\Delta h^*/R$ (kK)	m
300	0.073	0.42	47.0	−22.8	0.3074	74.02	87.38
400	0.062	0.42	38.6	−25.7	0.30386	70.82	83.60
450	0.063	0.41	35.5	−27.3	0.30305	71.34	84.22
500	0.062	0.42	32.5	−28.8	0.30176	71.59	84.52
550	0.062	0.42	29.6	−30.2	0.30021	71.69	84.63
600	0.061	0.42	26.8	−31.5	0.30148	71.68	84.63
650	0.061	0.42	24.1	−32.7	0.2986	71.63	84.57
700	0.060	0.42	21.6	−33.9	0.2946	71.77	84.73
800	0.061	0.43	17.0	−36.2	0.2906	72.24	85.28
900	0.059	0.44	12.3	−38.1	0.28632	71.88	84.86
1000	0.059	0.44	8.1	−40.0	0.28213	71.97	84.96
1500	0.056	0.45	−10.5	−47.8	0.26254	71.50	84.41

contrary the other six thermograms are well described with the same set of parameters. This is not an indication that the model equations describe better some specific thermal histories, the thermograms G, H and I can be well reproduced but with a set of model parameters which would be slightly different than the set obtained in the simultaneous fit of the nine thermograms. This introduces an uncertainty in the determination of the model parameters and the aim of this work is to study this uncertainty.

The curves calculated with the other sets in Table 1, i.e., with different values of B exactly superposes on the curves shown for $B = 550$ J/g, and as a consequence the value of the objective function is nearly the same for all of them. In fact EC slightly decreases as the value of B increases. From the set of parameters it is possible to calculate the temperature dependence of the relaxation times in equilibrium, obtained by substitution of Eq. (7) into Eq. (3). As shown in Fig. 3 the relaxation times in equilibrium calculated from different sets of parameters of Table 1 are also equal to each other while they are in the order of magnitude which is significant for these experiments, although they start deviating from each other at relaxation times below 0.01 seconds. The correlation between B and T_2 is quite apparent: the latter decreases as B increases. Some additional information is needed to determine the value of one of these parameters independently. This information may come from additional experiments or theoretical arguments. For example experimental data similar to thermograms G to I allow to determine the dependence of the glass transition temperature measured in the heating scan on the cooling rate q^-. It has been shown that

$$\frac{\partial \ln \tau^{eq}}{\partial 1/T} = -\frac{\partial \ln q^-}{\partial 1/T_g} = \frac{\Delta h^*}{R} \tag{10}$$

this relationship has been frequently used to calculate the apparent activation energy Δh^* of the Narayanaswamy–Moynihan [3,4] model. Nevertheless, as shown in Table 1,

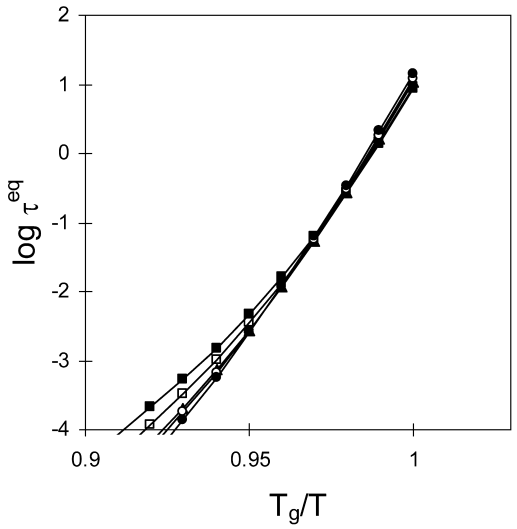

Fig. 3. Temperature dependence of the relaxation time in equilibrium (calculated with Eqs. (3) and (7)) with $B = 400$ J/g (■), $B = 550$ J/g (□), $B = 800$ J/g (▲), $B = 1000$ J/g (○) and $B = 1500$ J/g (◆) and the rest of model parameters according to Table 1.

the differences in the values of $\Delta h^*/R$, the right hand term of Eq. (10), calculated with the different sets of parameters are not significant and the experimental datum of the left hand side of the equation cannot be used to discriminate between them.

A rough approximation can come from the values of T_2 or the pre-exponential factor A, the former should be around 50° below the glass transition temperature (the value of $T_g = 94.8$ °C was calculated from the scan measured after cooling at 20 °C/min as the mid point of the rise of the heat capacity in the transition) and the later should be around 10^{-14} s, i.e. $\ln A \approx -32$. These criteria allows to reject values of B higher than around 1000 J/g. In the rest of the work we will assume that a value for B can be fixed, we will take $B = 550$ J/g and we will present a way to characterise the uncertainty in the determination of the rest of parameters.

The procedure we propose to do that is to apply the curve fitting method to different sets of experimental curves and analyse statistically the values of the parameters found by the least squares search routine. Thus, for instance, with our set of nine experimental thermograms it is possible to select 126 different groups of 5 experimental curves, fit the model to any of them and analyse the scattering in the values of the parameters found. This procedure was followed with the 9 possible sets of one curve, 36 sets of two curves, 84 sets of three curves, 99 sets of 4 curves, 60 sets of 5 curves, 82 sets of 6 curves, 31 sets of 7 curves and 9 sets of 8 curves. Fig. 4 gives the average and standard deviation of each parameter as a function of the number of experimental thermograms included in the simultaneous fitting routine.

The uncertainty in the fitting parameters is highly dependent on the number of curves used in the fitting routine and clearly the fit to a single experimental

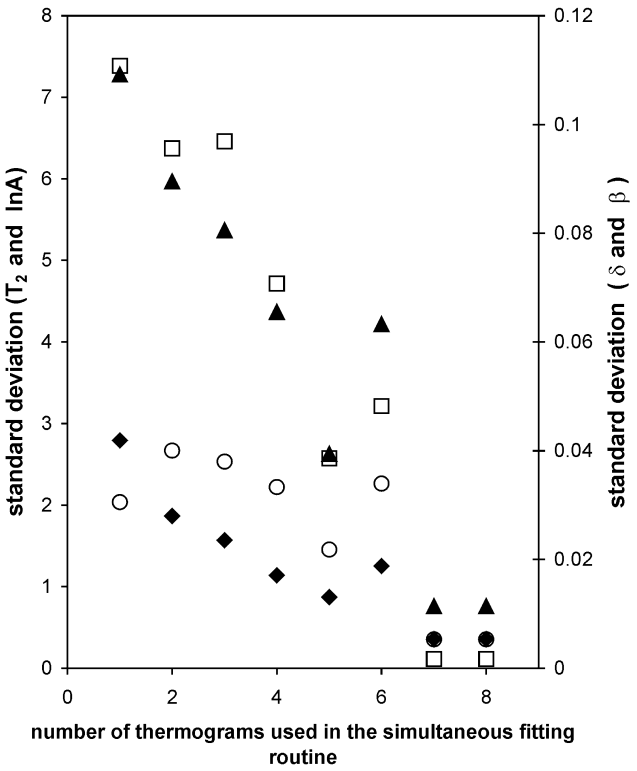

Fig. 4. Standard deviation of the parameters δ (◆), β (□), T_2 (▲) and $\ln A$ (○) as a function of the number of experimental thermograms simultaneously fitted in the least squares search routine.

thermogram is not representative at all of the material behaviour. There is a broad collection of sets of fitting parameters that are able to reproduce a single experimental thermogram with similar accuracy and as a consequence the least-squares routine stops in any of the many possible solutions. If the number of curves is 6 or more, the average values of the parameters are nearly constant and the standard deviation is the same when 7 or 8 curves are fitted simultaneously. Some points in Fig. 4 appear to fall out of the pattern of the rest of results. This was clearly due to the fact than in several fits the search routine failed to reach the minimum value of the error function. Nevertheless these points were not rejected and all the results were included in the statistical analysis.

If the uncertainty is calculated considering the fits using 8 thermograms, for $B = 550$ J/g, the values of the rest of parameters would be $\delta = 0.072 \pm 0.007$ J/g K, $\beta = 0.420 \pm 0.002$, $T_2 = 32.2 \pm 1.4$ °C, $\ln A = -31.6 \pm 0.7$ s. The nine sets of parameters obtained are included in Table 2. The value of δ is around a 28% of the configurational heat capacity what means that the $S_c^{lim}(T)$ line is significantly different from $S_c^{eq}(T)$ at temperatures below the glass transition.

The uncertainty in the relaxation times calculated by the model equations and through them the uncertainty in other important parameters as the apparent activation energy in equilibrium at T_g or the fragility parameter can also be obtained. The relaxation time was calculated with the different sets of parameters included in Table 2. From the $\tau(T)$ curves calculated for the heating scan measured in a sample that was previously cooled from equilibrium at 20 °C/min (Fig. 5), we determined the apparent activation energy both in the glassy state,

$$\mathrm{Ea}_g = R\frac{\partial \ln \tau^g}{\partial 1/T},$$

where τ^g is the relaxation times calculate at low temperature, between 70 and 85 °C, in the glassy state and R is the gas constant. The apparent activation energy Δh^* in equilibrium at T_g was also calculated using Eqs. (3) and (7) and the fragility parameter [35]

$$m = \left.\frac{\partial \ln \tau^{eq}}{\partial T_g/T}\right|_{T_g}$$

The mean values and standard deviations were calculated from the set of nine values corresponding to Table 2. The absolute value of the relaxation time in equilibrium at the glass transition temperature was also considered. The results are $\Delta h^*/R = 75.6 \pm 3.3$ kK, $m = 89.2 \pm 3.9$, $\mathrm{Ea}_g = 18.7 \pm 0.2$ K^{-1}, $\tau^{eq}(T_g) = 10.9 \pm 1.0$ *s*.

This calculation has been performed considering that B can be evaluated independently from the series of experimental thermograms, but it is interesting to note that even in the case that B is not precisely determined, the uncertainty in the values of the relaxation times is still acceptable. To show this point the same procedure explained above was followed with the different sets of parameters in Table 1 corresponding to values of B between 400 and 1500 J/g. The Ahrrenius plots showing the evolution of the relaxation time during the scan is

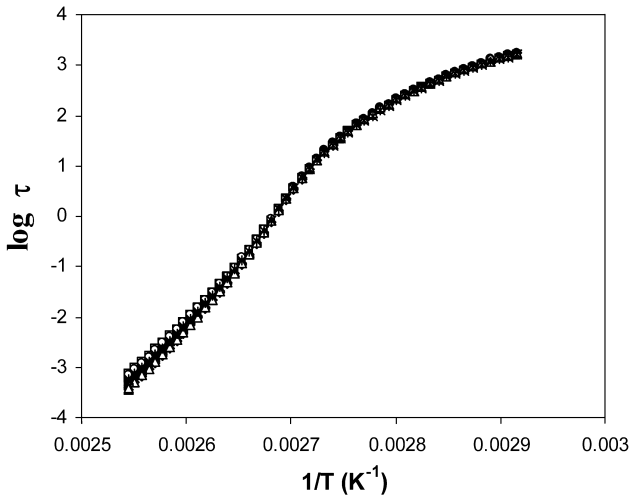

Fig. 5. Temperature dependence of the relaxation time calculated with the model equations for a heating scan at 20 °/min after cooling the sample at 20 °/min from equilibrium. Nine curves has been represented, calculated with the parameters determined by the least squares routine conducted with the nine posible sets of eight thermograms (Table 2).

Table 2
Model parameters (δ, β, T_2, ln A) found by curve fitting of the nine possible different sets of eight experimental thermograms. The value of B was always 550 J/g. The value of the error function (EC), the apparent activation enthalpy in equilibrium at T_g ($\Delta h^*/R$) and the fragility parameter (m) are also included

Set of eight experimental thermograms	δ	β	T_2 (°C)	Ln(A/s)	EC	$\Delta h^*/R$ (kK)	m
1	0.072	0.4216	32.159	−31.556	0.2643	77,87	91.93
2	0.075	0.4223	32.234	−31.542	0.2982	78,06	92.16
3	0.057	0.4188	28.899	−29.8423	0.2843	70,12	82.78
4	0.074	0.4162	32.294	−31.565	0.2889	78,22	92.34
5	0.063	0.4215	29.457	−30.068	0.2748	71,36	84.25
6	0.077	0.424	32.397	−31.596	0.2755	78,48	92.66
7	0.076	0.4234	32.322	−31.565	0.2700	78,29	92.43
8	0.067	0.4217	30.476	−30.607	0.2481	73,72	87.03
9	0.068	0.4227	30.592	−30.669	0.2381	73,99	87.36

represented in Fig. 6. The results are now $\Delta h^*/R = 71.8 \pm 7.7$ kK (as was already mentioned above), $m = 84.8 \pm 0.91$, $\tau^{eq}(T_g) = 10.2 \pm 1.6$ s. The apparent activation energy seems to increase with increasing B at least for values of B higher than 500 J/g, considering all the values of table one an estimation of $Ea_g = 19.1 \pm 1.3\ K^{-1}$.

4. Conclusions

The determination of the relaxation times of the structural relaxation process from the experimental DSC thermograms can be quite accurate if a series of thermograms measured after different thermal histories are available. The curve fitting should be conducted simultaneously to a significant set of these thermograms. It makes no sense to fit the model equations to a single thermogram. There is a strong correlation between the parameters B and T_2, which comes from the correlation existing in the corresponding parameters in the Vogel equation. This implies that some additional information is necessary to obtain precise values of any of these parameters, nevertheless this problem does not invalidate the calculation of the relaxation times.

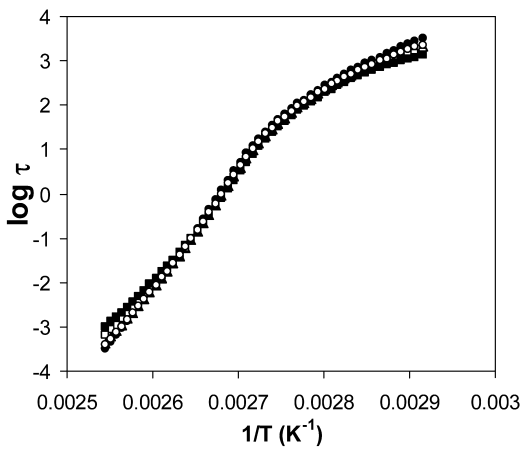

Fig. 6. Temperature dependence of the relaxation time calculated with the model equations for a heating scan at 20°/min after cooling the sample at 20°/min from equilibrium with $B = 400$ J/g (■), $B = 550$ J/g (□), $B = 800$ J/g (▲), $B = 1000$ J/g (○) and $B = 1500$ J/g (◆) and the rest of model parameters according to Table 1.

References

[1] Vogel H. Phys Z 1921;22:645.
[2] Fulcher GA. J Am Ceram Soc 1925;8:339.
[3] Tamman G, Hesse W. Z Anorg Allg Chem 1926;156:245.
[4] Narayanaswamy OS. J Am Ceram Soc 1971;54:491.
[5] Moynihan CT, Macedo PB, Montrose CJ, Gupta PK, DeBolt MA, Dill JF, Dom BE, Drake PW, Esteal AJ, Elterman PB, Moeller RP, Sasabe H. Ann NY Acad Sci 1976;279:15.
[6] Kovacs AJ, Aklonis JJ, Hutchinson JM, Ramos AR. J Polym Sci, Polym Phys Ed 1979;17:1097.
[7] Scherer GW. J Non-Cryst Solids 1990;123:75.
[8] Hodge IM. Macromolecules 1987;20:2897.
[9] Hodge IM. J Non-Cryst Solids 1994;169:211.
[10] Hutchinson JM. Prog Polym Sci 1995;20:703.
[11] Gómez Ribelles JL, Monleón Pradas M. Macromolecules 1995;28:5867.
[12] Meseguer Dueñas JM, Vidaurre Garayo A, Romero Colomer F, Más Estellés J, Gómez Ribelles JL, Monleón Pradas M. J Polym Sci, Polym Phys Ed 1997;35:2201.
[13] Prest WM, Roberts Jr FJ, Hodge IM, Proc NATAS. Conf 12th 1980;119–23.
[14] Hodge IM, Huvard GS. Macromolecules 1983;16:371.
[15] Tribone JJ, O Reilly JM, Greener J. Macromolecules 1986;19:1732.
[16] Gómez Ribelles JL, Ribes Greus A, Diaz Calleja R. Polymer 1990;31:223.
[17] Moynihan CT, Crichton SN, Opalka SM. J Non-Cryst Solids 1991;131–133:420.
[18] Oudhuis AACM, ten Brinke G. Macromolecules 1992;25:698.
[19] Hodge IM. J Non-Cryst Solids 1991;131–133:435.
[20] Mohynihan CT, Easteal AJ, DeBolt MA, Tucker J. J Am Ceram Soc 1976;59:12.
[21] Ramos AR, Hutchinson JM, Kovacs AJ. J Polym Sci, Polym Phys Ed 1984;22:1655.
[22] Hutchinson JM, Ruddy M. J Polym Sci, Polym Phys Ed 1988;26:2341.
[23] Hodge IM, O'Reilly JM. J Phys Chem B 1999;103:4171.
[24] Montserrat S, Hutchinson JM. Polymer 2002;43:351.
[25] Torregrosa C, Vidaurre A, Meseguer Dueñas JM, Salmerón M, Monleón Pradas M, Gómez Ribelles JL. Colloid Polym Sci 1999;277:1033.
[26] Gómez Ribelles JL, Monleón Pradas M, Vidaurre Garayo A, Romero Colomer F, Más Estelles J, Meseguer Dueñas JM. Polymer 1997;38:963.

[27] Gómez Ribelles JL, Vidaurre Garayo A, Cowie JMG, Ferguson R, Harris S, McEwen IJ. Polymer 1998;40:183.
[28] Alves NM, Mano J, Balaguer E, Meseguer Dueñas JM, Gómez Ribelles JL. Polymer 2002;43:4111.
[29] Montserrat S, Gómez Ribelles JL, Meseguer Dueñas JM. Polymer 1998;39:3801.
[30] Gómez Ribelles JL, Monleón Pradas M, Meseguer Dueñas JM, Privalko VP. J Non-Cryst Solids 1999;244:172.
[31] Mano JF, Alves NM, Meseguer Dueñas JM, Gómez Ribelles JL. Polymer 1999;40:6545.
[32] Adam G, Gibbs JH. J Chem Phys 1965;43:139.
[33] Gibbs JH, DiMarzio EA. J Chem Phys 1958;28:373.
[34] Hutchinson JM, Smith S, Horne B, Gourlay GM. Macromolecules 1999;32:5046.
[35] Böhmer R, Ngai KL, Angell CA, Plazek DJ. J Chem Phys 1993;99:4201.